

# Dynamics of fast ions produced from laser produced aluminum plasma

Garima Arora,<sup>1, a)</sup> Jinto Thomas,<sup>1</sup> and Hem Chandra Joshi<sup>1,2</sup>

<sup>1)</sup>*Institute For Plasma Research, Bhat, Gandhinagar, Gujarat, 382428, India*

<sup>2)</sup>*Homi Bhabha National Institute, Training School Complex, Anushaktinagar, Mumbai, 400094, India*

(Dated: 24 March 2022)

In this work, dynamics of multi-charged ions emitted from an aluminum plasma produced by Q switched Nd:Yag laser is studied using time of flight (TOF) measurements from Langmuir Probe (LP) and spectroscopy (STOF) under Ar ambient of 0.02 mbar. The temporal evolution of multi-charged ions, background neutrals and ions is systematically studied for varying laser intensities. The temporal evolution shows all the species have dual peak structure for all the laser energies considered in the study. The fast peak is sharp whereas the slow peak is broad similar to that observed in previous studies. Moreover, higher charged ions have higher velocity, indicating acceleration from the transient electric field produced at the very initial temporal stages of expansion. Interestingly, the fast peak gets delayed, whereas the slow peak advances in time with increased laser intensity, which has not been reported in earlier studies. The observations point towards the possible role of ambipolar electric fields in the unexpected observed behavior of the TOF profiles.

## I. INTRODUCTION

Study on the dynamics of fast ions from laser produced plasma has significant interest for inertial confinement fusion<sup>1</sup>, laser-matter interaction<sup>2,3</sup> and different accelerations mechanisms<sup>4,5</sup>. In the literature, various mechanisms of acceleration of ions have been reported, such as target normal sheath acceleration (TNSA)<sup>6,7</sup>, backward plasma acceleration (BPA)<sup>8</sup>, radiation pressure acceleration (RPA)<sup>9,10</sup>, double layer formation (DL)<sup>11</sup> depending upon the laser intensity.

The energy distribution of ions observed far away from the target may be divided into two parts; (1) low energy ions comprising of ablated mass and (2) a smaller fraction of energetic, fast ions. These fast ions from laser produced plasma form a significantly small group of ions that are the transporters of absorbed laser energy<sup>12</sup>. It has been reported that the laser energy is deposited on the hot electron distribution, where these high-energy electrons impart their energy to accelerate the ions<sup>6,7</sup>. Hence, a systematic study of ion acceleration can be informative further in the understanding of laser-matter interaction.

Ion acceleration has been studied extensively in case of ultra-fast laser-plasma interaction<sup>6-8</sup>. Interaction of nanoseconds (ns) laser pulse and evolution of ns laser produced plasma in vacuum, and background gas has also been reported<sup>13,14</sup>. Acceleration of ions in ns plasma due to ambipolar electric field originated from DL structures has been reported<sup>11,15</sup>. DL is formed by the spatial charge separation in the expanding plasma and consequently breaking the quasineutrality condition. Thus, DL modifies the velocity distribution of ions into fast and thermal ions.<sup>11,16,17</sup>

Dual peak distribution of electrons and ions measured in time of flight studies is well reported. Issac *et. al.*<sup>18</sup>

observed twin peak structure in the time of flight measurement of electron distribution. These prompt electrons ionize the background gas because of their higher energy. Verhoff *et. al.*<sup>19</sup> reported the generation of dual peak structure with fast ions having a kinetic energy of sub-keV using fs laser pulse. Bulgakawa *et. al.*<sup>11</sup> explained the origin of the double-peak structure in ion collector time of flight distribution (TOF) for both vacuum and background gas due to self-generated ambipolar electric field (DL). Wu *et. al.*<sup>16</sup> studied the dynamics of multi-charged ions emitted from ns laser produced molybdenum plasma from mass spectrometry. They observed multi peaks structures in time-resolved mass spectroscopy and linked the velocities of multi-charged ions to the acceleration in the transient sheath. Kelley *et. al.*<sup>20</sup> performed experiments to measure ion distribution for different materials using ultrafast laser for various laser intensities. They proposed a bi-modal TOF distribution to explain the double peak structure in time of flight measurements. Also, they have reported linear increase in the energy of slow peaks with laser fluence. However, the fast peaks change from sublinear to superlinear with laser fluences depending upon the atomic mass of the target. Elsieid *et. al.*<sup>12</sup> studied the dependence of charge state and angular distribution of ion profiles using FC in an ultrafast laser generated plasma. They have also observed dual peak character in TOF, where the origin of the fast peak is ascribed to ambipolar electric field, and the slow peak is ascribed to thermal vaporization. The dynamics of fast and slow peaks are well studied in case of ultrafast lasers also. Batool *et. al.*<sup>17</sup> observed two distant peaks of ions with a time delay of nanoseconds and microseconds. They have observed that the density of slow ions is 12 times higher than the density of fast ions, and the kinetic energies of fast and slow ions increase with laser irradiances. Dogar *et. al.*<sup>21</sup> measured ion flux from TOF ion collector for various metals using ns laser pulse. They have observed two groups of fast ions. They claimed that early fast peak is present for every metal and attributed it to surface contamination. The second

<sup>a)</sup>Electronic mail: [garimagarora@gmail.com](mailto:garimagarora@gmail.com)

group is due to ion acceleration from the prompt electron emission and found only in heavier metals. Bhatti *et. al.*<sup>22</sup> suggested that self generated electric field (SGEF) is responsible for fast ions. They observed increase in SGEF increases with laser irradiance. Farid *et. al.*<sup>23</sup> reported enhancement in kinetic energy of fast and slow ions with increase in laser fluence which saturates at higher fluence. Wu *et. al.*<sup>16</sup> reported the saturation of kinetic energy of molybdenum ions with laser intensity.

Despite these works, concerted study of the time evolution of various charge states appears to be quite challenging. Hence, in this work we have systematically studied the effect on the charge states and background argon in laser produced aluminum plasma from LP and STOF at a background pressure of 0.02 mbar of argon ambient. Dual peak structure is observed in temporal evolution from both the diagnostics. Multi-charged ions exhibiting the dependence on arrival time is also observed. Further, highly charged ions gain higher velocity due to ambipolar electric field, however, get delayed with increase in laser intensity. The TOF results also show that fast ions are delayed with increase in laser intensity. This peculiar behavior is attributed to decrease in the electric field. The paper is divided in the following sections. Sec II gives the details of the experimental setup, laser and plasma diagnostics used to investigate dynamics of fast ions. Sec III describes the observations and discussion. Concluding remarks are in Sec. IV.

## II. EXPERIMENTAL SET-UP

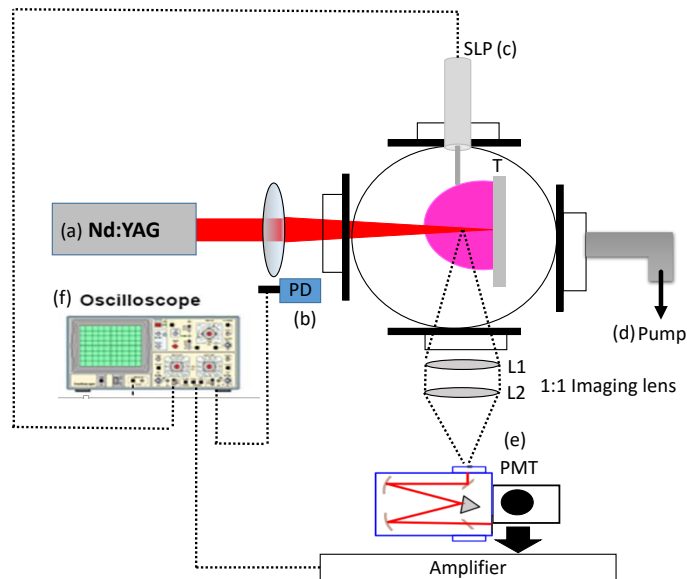


FIG. 1. Schematic diagram of experimental set-up. (a) ND:YAG laser, (b) PD photodiode (c) LP single Langmuir Probe (LP) (d) Rotary Pump (e) Phot Multiplier Tube (PMT) (f) Fast Digital Oscilloscope and (g) L1 and L2 lens system.

Fig.1 shows the schematic diagram of the experimental set-up used to study the dynamics of ions using LP and STOF. A Q switched Nd:YAG laser (wavelength  $\lambda = 1064nm$ , pulse width  $\tau = 8ns$ ) is used to ablate the target and produce plasma. The energy of laser is varied from 100 mJ to 930 mJ and is focused on the sample using a 25 cm plano convex lens. The spot size on the sample is fixed to  $\sim 1mm$  so that laser intensity is  $3-24 GW/cm^2$ .

A cylindrical glass chamber of 100 mm diameter and 600 mm length serves as vacuum chamber which is evacuated by a rotary pump. The chamber is filled with argon gas to set the desired working pressure. Various diagnostics such as LP, STOF, 1 m long Czerny-Turner spectrograph coupled with ICCD, and fast imaging with different narrow-band interference filters are used for studying the fast and slow dynamics of plasma plume. Other ports are used to mount the gas feeding valve to set the working pressure. A pirani gauge for measuring the pressure in the chamber.

A well polished and cleaned aluminum strip mounted on a vacuum compatible translation stage is used as the target for laser produced plasma. The translation stage is moved after each laser pulse so as to ablate from fresh spot on the sample to maintain the experimental conditions same and multiple acquisitions are performed for each experiments to reduce the statistical error.

LP is made of tungsten wire having a diameter of 1 mm and length 10 mm. The probe is negatively biased to -30 V using a  $50 \Omega$  resistance, and current is measured using a (5V/A) current transformer. The probe is mounted on an another translation stage to position it accurately at the desired distance from the sample perpendicular to the plasma plume propagation. The STOF diagnostics is integrated with the experimental setup using a high-resolution monochromator (Hr460) coupled with a fast photo-multiplier tube (PMT) (R943-02 Hamamatsu). The PMT output is connected to a buffer amplifier and fed to a fast digital oscilloscope to record the temporal evolution. An imaging system comprising of two lenses with 1:1 magnification is used to feed the emission from the plasma plume into an optical fiber. Again LP and STOF data are averaged over five plasma shots to reduce the statistical uncertainty in the measurements.

## III. RESULTS AND DISCUSSION

### A. Time of Flight Measurements

The time evolution of ion saturation current measured from LP for four different laser intensities at a background pressure of  $\sim 0.02$  mbar is shown in Fig. 2. As can be seen the ion signal has two prominent peaks. The first peak observed at a delay of 100 ns is due to the fast ions generated from the laser plasma. The fast ions can be attributed to accelerated ions from the elec-

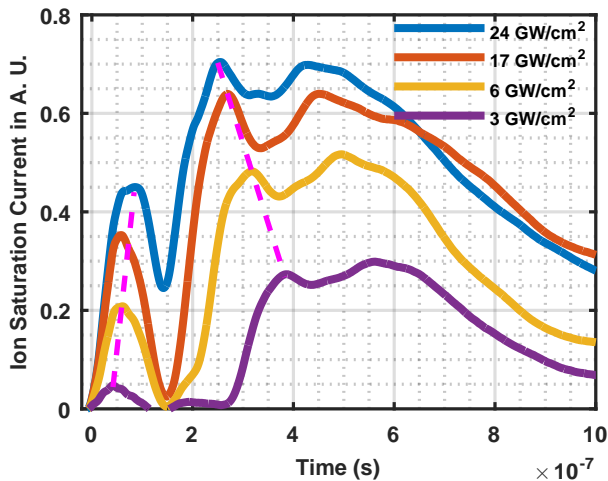


FIG. 2. Temporal evolution of ion saturation current of plasma plume for four different laser intensities recorded at 30 mm from the target. The plasma plume expands into argon background pressure of 0.02 mbar. The dotted pink lines are formed by joining the peaking time of ion current profile to mark the evolution of peaking times of fast and slow ions.

tric field developed by the loss of electrons at the initial times as reported in earlier works which are further explained in terms of double layer formation<sup>11</sup>. In nanosecond laser generated plasma, the leading portion of the laser pulse heats, melts, and vaporizes the target forming a vapor cloud. The trailing part of the laser pulse is absorbed by this vapor cloud which is mainly by inverse bremsstrahlung (IB) process. When the laser energy increases, the atoms or ions get ionized further due to electron impact ionization leading to the generation of multiple charge states. As the electrons gain large kinetic energy from the laser, they escape from the target. The loss of these highly energetic electrons leads to charge separation and creates self-generated electric field leading to quasi neutrality violation. These ions which get accelerated from this electric field and acquire higher kinetic energy are believed to be responsible for the fast peak observed from the LP. The second prominent peak which is broad and extends beyond  $1 \mu\text{s}$  corresponds to ions originating from slow thermal process. Fig. 2 also shows that ion saturation current increases with increase in laser intensities which is in line with earlier reported measurements from ion saturation current<sup>17</sup>.

However we would like to mention that a very interesting and unique observation here is that the fast peak appears to be delayed as the laser intensity increases whereas, the slower peak becomes faster. For clarity a pink dotted line marks the variation of peaking time of the fast and slow peaks of ion saturation current. As mentioned earlier, previous studies from Faraday cup<sup>17,22</sup> and LP<sup>24,25</sup> reported that the fast and slow peaks of ion current get faster with laser intensity<sup>17,22</sup> and finally become stagnant.<sup>16</sup> On the contrary in our case, the fast ions slow down as the laser intensity increases.

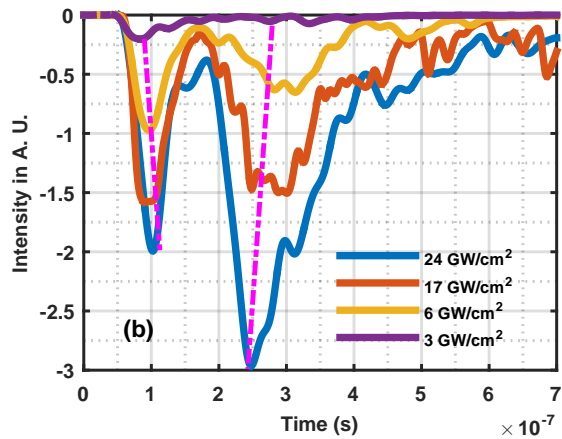
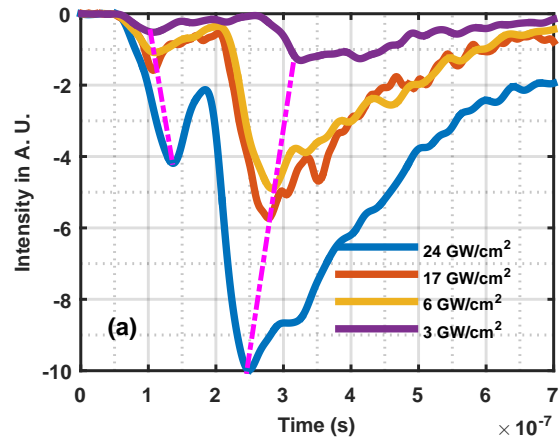


FIG. 3. STOF profiles of (a)  $Al^{1+}$  (358.7 nm) ionic line and (b)  $Al^{2+}$  (451.3 nm) ionic line for four different laser intensity. The argon pressure is 0.02 mbar. The profiles are recorded at 30 mm from the target.

To understand the behavior of peaking time of the fast peak of ion saturation current with laser intensity, STOF experiments are performed for different ionic species. Fig. 3(a) and (b) show the STOF profiles of  $Al^{1+}$  and  $Al^{2+}$  ionic emission lines for four different laser intensities. Similar to the ion saturation current recorded from LP, the STOF profile of these charge states also show a double peak structure with narrow fast peak and a broad slow peak with increasing amplitude with increase in laser intensity. As can be seen from the figure, the behavior of peaking time, marked with the pink dotted line, is similar as in case of ion saturation current (Fig.2) recorded using the LP. The fast peak gets delayed, whereas the slow peak becomes faster as laser intensity increases for both  $Al^{1+}$  and  $Al^{2+}$ . The STOF profiles for both these charged species show similar trend in peaking time of fast and slow peaks as in case of ion saturation current recorded on the LP. This shows that the observed dynamics of ion saturation current indeed holds with individual charge species as well.

To further investigate the plasma evolution, the tempo-

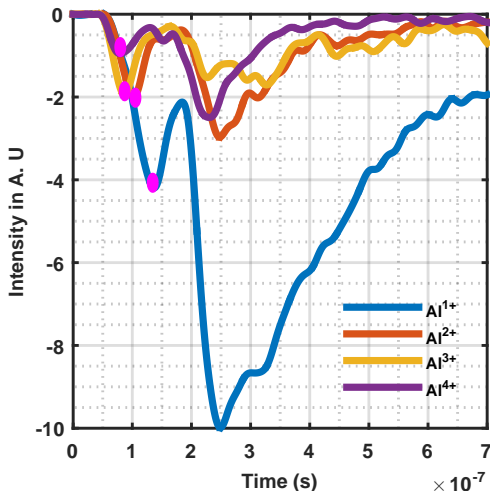


FIG. 4. STOF ionic profile of  $Al^{1+}$  (358.7 nm),  $Al^{2+}$  (451.3 nm),  $Al^{3+}$  (351.7 nm),  $Al^{4+}$  (338.1 nm) where the plume is formed by setting laser intensity  $24 \text{ GW/cm}^2$  at background pressure of 0.02 mbar. The profiles are recorded at 30 mm from the target.

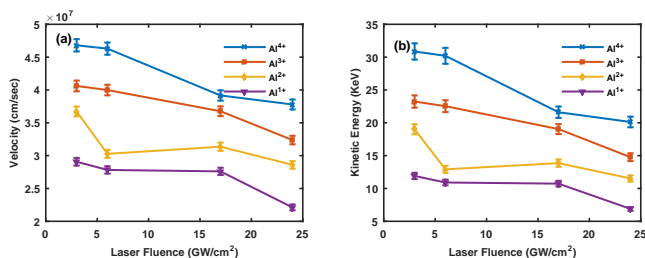


FIG. 5. (a) Velocity (b) Kinetic energy of fast ions of  $Al^{n+}$  charged species as a function of laser intensity estimated from the fast peak of STOF profile of  $Al^{n+}$  ionic lines. The background pressure is set to 0.02 mbar and STOF profiles are recorded at a distance 30 mm away from the target.

ral behavior of different charge states of aluminum species produced for laser power intensity of  $24 \text{ GW/cm}^2$  and background  $\sim 0.02$  mbar is compared in Fig.4. It is observed that both the fast and slow components of the higher charge state reach earlier as compared to respective components of lower charge states indicating that the higher charge state acquire higher velocity. The enhanced velocity for higher charge state has been reported earlier and explained using the double layer<sup>11,16</sup> concept where the highly charged species are expected to have larger acceleration and attain higher velocity.

Fig. 5 (a) and (b) show the trend of velocities and kinetic energies of different charged species as a function of laser intensity. The velocity of charged species is estimated from the peaking time from respective STOF profiles and subsequently kinetic energies are estimated. As can be seen from figure 5 velocity of all the charged

species decreases with an increase in laser intensity. However, for a particular laser intensity, the velocity and hence kinetic energy for higher charge state is higher than that for lower charged ions. This again indicates that the dynamics of charged states should be governed by the electric field in the early stages of the plasma formation.

The ion saturation current recorded by LP is expected to have contribution from all the charged states of ions. Fig. 6 (a) (up to 200 ns) and Fig. 6(b) (from 200 ns to  $2 \mu\text{s}$ ) show the evolution of fast and slow peaks of ion saturation current and the STOF profiles of individual charge states of aluminum and argon respectively. The plots are normalized to the peak value of the respective species for convenient comparison. The solid blue line is the probe current, whereas the STOF emission profiles from  $Al^{1+}$ ,  $Al^{2+}$ ,  $Al^{3+}$ ,  $Al^{4+}$ ,  $Ar^{1+}$  are plotted with markers joined with lines. One can notice that all the charged species contribute to the fast peak (shown in Fig.6(a)). The contribution to the ion saturation current is expected to be dominated by the charge states of aluminum rather than argon, considering the lower ambient pressure and dense aluminum plasma. As a result ambient Ar is likely to be pushed outwards. However, as can be seen from figure6(a)  $Ar^{1+}$  is present at the same time scale as that of aluminum ( $Al^{4+}$ ) ions. The fast Ar ions can not be inherently present in the plasma plume because in this case they should reach at a later time than  $Al^{1+}$  due to its heavier mass. As will be discussed latter, it is also evident from images that Ar does not constitute the main plasma plume but is present at the boundary (shown in Fig.9). The most probable reason for the presence of  $Ar^{1+}$  in the same timescale of the fast peak of aluminum higher charge states appears to be a some kind of collisional process with highly charged states of aluminum. Also, it is evident from the figure that the ion saturation current is significant even at shorter time scales than the recorded evolution of charge states, which indicates that possible higher charge states higher charge states (not recorded from STOF) may be present.

The slow peak of LP is broad and appears as a convolution of multiple peaks merged together, reaching at 3 cm around 300 ns, and persisting up to  $1 \mu\text{s}$  shown in Fig.6(b). Here also, all the charged species are likely to contribute to the ion saturation current, and the first peak of the slow peak is precisely coinciding with the slow peaks of  $Al^{1+}$  and  $Al^{2+}$ . The second slow peak is likely to be the contribution of all the aluminum ions and also background ions.

To investigate whether the observed delay in the fast peak with laser intensity is only for charged species, the time evolution of emission from  $Al^*$  (396.2 nm) line emission for four different laser intensities is plotted in Fig. 7. It is to be noted that prominent double peak structure is present in case of aluminum neutrals also. Akin to aluminum ions, emission intensity increases with laser

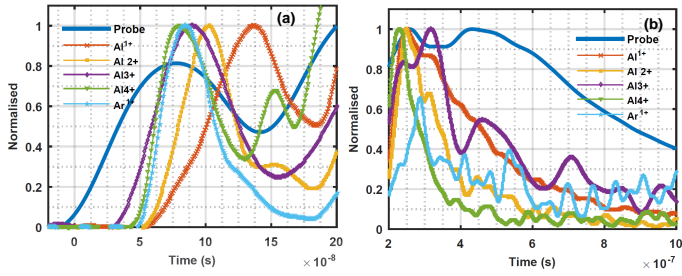


FIG. 6. Temporal evolution of normalized ion saturation current from LP as well as the normalized STOF from ionic species  $Al^{1+}$ ,  $Al^{2+}$ ,  $Al^{3+}$ ,  $Al^{4+}$   $Ar^{1+}$  to show the contribution of each charged species towards the ion current upto 200 ns (a) and from 200 ns to 1  $\mu$ s (b). The plume is formed at 24  $GW/cm^2$  laser intensity with ambient argon pressure of 0.02 mbar. Ion current as well as STOF are recorded at 30 mm from the target.

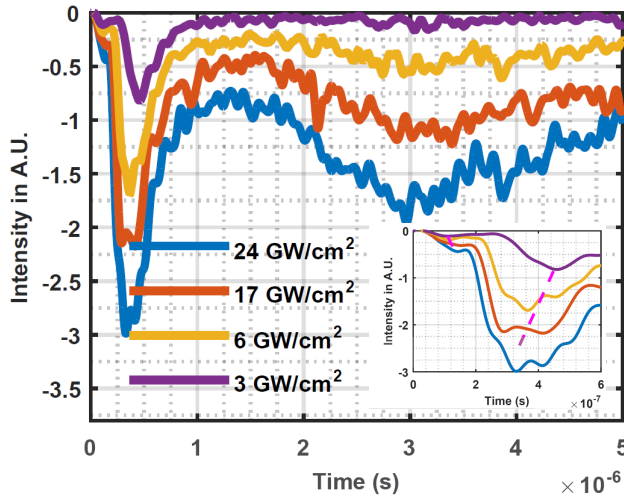


FIG. 7. STOF profile of  $Al^*$  (396.2 nm) line for four different laser intensities. The ambient argon pressure is 0.02 mbar. The profiles are recorded at 30 mm from the target. Inset shows the STOF upto 600 ns to show the trend of fast and slow peaks with laser intensity.

intensity. However, as can be seen from Fig. 7 (shown in the inset), the fast peak at around 160 ns (for low intensity) and the slow peak at 250 ns again shows unexpected behavior with laser intensity. The peaking time of fast peak becomes longer with laser power intensity similar the case of charged aluminum species. However, the slow peak advances with the increase in laser power intensity. The fast and slow neutrals are likely to be formed by the recombination from fast and slow ions of  $Al^{1+}$  ions respectively, and hence they appear to follow a similar trend as exhibited by aluminum ions with intensity. Also it can be seen from the figure that STOF for neutral shows a relatively broad peak at around 3  $\mu$ s. However, no emission from ions or significant ion saturation current is observed in this time range. As mentioned the emission from aluminum neutrals is likely to originate from

the recombination from Al ions as the plasma temperature decreases with time. Further, the peaking time of the broad peak is delayed as the laser intensity increases. This is because at initial stages the plasma temperature is higher at higher laser intensity, and the plume lifetime is longer. Here more ionization is expected resulting in increased charge states. However, the recombination process can occur at longer times when temperature is decreased substantially.

The time profiles of fast and slow peaks of Ar neutrals

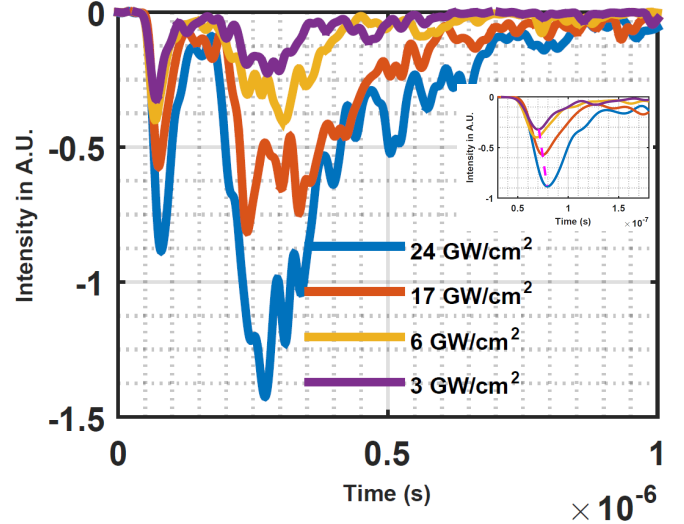


FIG. 8. STOF profile of  $Ar^*$  (420.1 nm) line for four different laser intensities. The argon pressure 0.02 mbar. The profiles are recorded at 30 mm from the target. Inset shows the STOF upto 800 ns to demonstrate the trend of fast and slow peaks with laser intensity.

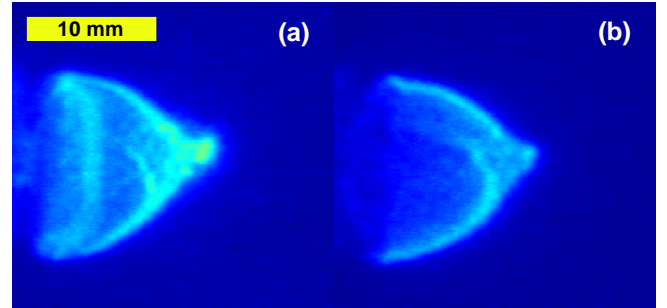


FIG. 9. ICCD images of (a)  $Al^{1+}$  (466.3 nm) (b)  $Ar^{1+}$  (434.8 nm) with a delay of 100 ns for an integration time of 5 ns at 0.5 mbar argon pressure.

with an increase in laser intensity are also shown in Fig. 8. One can notice that emission from background argon neutrals persists upto 700 ns in contrast to Al neutrals exhibit emission up to 6  $\mu$ s. It is interesting to see that the STOF profiles of Ar neutrals also show similar trend as that of Al ions. The fast peak from Ar neutral appears around 90 ns where Al ions with higher charge states are

present, and hence it is expected that these neutral may be excited by the some kind of collisional process with highly charged aluminum ions although excitation by fast electrons can not be ruled out. Moreover, the ions show delay in peaking time with intensity and interestingly the fast peak of Ar neutrals appears to follow the same trend.

To find out the possibility of the ambient Ar penetrating the plasma plume, we have recorded the temporal images of both singly charged aluminum and argon ions. In order to have significant emission from argon ions, the images are recorded at 0.5 mbar argon ambient. Fig. 9 (a) and (b) show the ICCD images of aluminum and argon ions at a time delay of 100 ns, respectively. It is clearly observed from the images that the contribution of emission in case of  $Al^{1+}$  is present in the main plasma plume and its boundary (near to the shock region). However, in case of  $Ar^{1+}$  the emission intensity is confined only to the boundary (periphery) of the plume. This further supports the fact that the background ions do not constitute the plasma plume and are present at the boundary. Further, these are excited by the electron or ion impact processes.

Briefly, from the present work, it is clearly evident that the velocity of fast ions decreases with an increase in laser intensity. Here, it is anticipated that the faster peak arises due to self generated electric fields at initial stage of plasma formation must become larger for higher laser intensity and there should be increase in the velocity of the charged species depending upon the charge. Interestingly, an opposite trend is observed in the present experiments. Here we would like to mention that in an earlier work, Wu *et. al.*<sup>16</sup> found that there is a decrease in the kinetic energy of  $Mo^{+1}$  ions as the laser intensity increases, which, however, is not observed for higher charge states in our work. They tentatively suggested that this behavior is likely to occur due to more collisions and recombinations during the expansion process. They also attributed the decrease in kinetic energy with intensity due to plasma shielding and absorption. In fact, the present experiments have also comparable laser intensity. From a simple comparison a similar reason can be expected for this observed reduction in kinetic energy of aluminum charge states. However, we would like to mention that in our case we have observed decrease in energy for all the studied charged states. Hence it can not be pointed out if there is any substantial evidence of the role of recombination processes.

Another possibility for this decrease in velocity is the decrease in the field strength at the early stages of plasma formation. It can be expected that the initial plasma plume density in the self regulating regime<sup>26</sup> may restrict the plasma density to the maximum of critical density equivalent to the laser frequency irrespective of the laser intensity. However, the possibility of increased temperature due to IB is more for the higher laser intensities. Hence it can be anticipated that during the interaction of laser pulse with the sample, the plasma density remains the same but the temperature increases as the laser inten-

sity increases. In case of such a scenario the Debye length of plasma plume will be larger for the plasma formed with higher laser intensity. As the thickness of the double layer formation depends on the Debye length, there is a possibility that the electric field strength may be weakened with higher laser intensity, and subsequent decrease in the velocity of charged species is expected.

Third possibility is the presence of bipolar nature of SGEF with opposite polarities as reported in some recent studies<sup>17,22</sup>. With increase in intensity, the balance between these fields with opposite polarities is likely to be disturbed and hence decrease in the velocities of charged species is possible. Here it can be mentioned that for correctly ascertaining the observed anomaly in the velocity of charged species, more insights into the plasma parameters and hence electric fields at the very early stage of plasma is needed. As the electric field can only be present within the Debye length, the density and temperature of plasma at the very initial stages of expansion is crucial. However, the existing diagnostics are not capable to get the plasma parameters at the very early stages of expansion. Though a clear cut explanation for the observed behavior can not be given at present, we believe the present work points towards peculiar behavior of fast ions which may lead to further investigations in this direction.

#### IV. CONCLUSIONS

The dynamics of fast and slow ions is studied for different laser intensities using LP and STOF. The ion current from LP shows a dual peak structure where the first peak is sharp and peaks around 100 ns. However, the slow peak is broad with peaking time around 400 ns. The ion current increases with laser intensity and the slow peak advances in time for higher laser intensity, similar to earlier reported works using ion collector current from FC. However in the present study, the fast peak shows somewhat peculiar behavior with laser intensity i.e it gets delayed in time with increase in laser intensity. Further, ion saturation current which can be assumed as the convolution of the contributions from all the charged species and confirms the anomaly in the fast peak. STOF profiles of all the charged species show similar trend as observed in case of LP. The dual peak nature is present in case of higher charged species in which fast peak is narrow and slow peak is broad. The decrease in velocity and hence kinetic energy is also observed in STOF as in case of LP. The energy of fast ions is the range of 10-40 KeV. The higher charged species have higher velocity as compared to lower charged species, which confirms the presence of a transient electric fields. Another interesting aspect is the dynamics of the background argon in the expanding plume. Though more detailed investigations of the early stages of plume expansion are required for getting finer aspects of the mechanism, we believe the present study brings out some hitherto not explored interesting

features regarding the species present in laser produced plasma plume in the presence of ambient argon.

## DATA AVAILABILITY

The data that supports the observations of this study are available from the corresponding author upon reasonable request.

## V. REFERENCES

- <sup>1</sup>H. Hora, “New aspects for fusion energy using inertial confinement,” *Laser and Particle Beams* **25**, 37–45 (2007).
- <sup>2</sup>T. Tajima and G. Mourou, “Zettawatt-exawatt lasers and their applications in ultrastrong-field physics,” *Physical Review Special Topics-Accelerators and Beams* **5**, 031301 (2002).
- <sup>3</sup>H. Daido, M. Nishiuchi, and A. S. Pirozhkov, “Review of laser-driven ion sources and their applications,” *Reports on progress in physics* **75**, 056401 (2012).
- <sup>4</sup>F. Amiranoff, S. Baton, D. Bernard, B. Cros, D. Descamps, F. Dorchies, F. Jacquet, V. Malka, J. Marques, G. Matthieussent, *et al.*, “Observation of laser wakefield acceleration of electrons,” *Physical Review Letters* **81**, 995 (1998).
- <sup>5</sup>P. Sprangle, G. Joyce, E. Esarey, and A. Ting, “Laser wakefield acceleration and relativistic optical guiding,” in *AIP Conference Proceedings*, Vol. 175 (American Institute of Physics, 1988) pp. 231–239.
- <sup>6</sup>M. Passoni, L. Bertagna, and A. Zani, “Target normal sheath acceleration: theory, comparison with experiments and future perspectives,” *New Journal of Physics* **12**, 045012 (2010).
- <sup>7</sup>J. Badziak, S. Głowacz, S. Jabłoński, P. Parys, J. Wołowski, H. Hora, J. Krása, L. Láska, and K. Rohlena, “Production of ultrahigh ion current densities at skin-layer subrelativistic laser-plasma interaction,” *Plasma Physics and Controlled Fusion* **46**, B541 (2004).
- <sup>8</sup>L. Láska, S. Cavallaro, K. Jungwirth, J. Krása, E. Krouský, D. Margarone, A. Mezzasalma, M. Pfeifer, K. Rohlena, L. Ryc, *et al.*, “Experimental studies of emission of highly charged anions and of x-rays from the laser-produced plasma at high laser intensities,” *The European Physical Journal D* **54**, 487–492 (2009).
- <sup>9</sup>A. Robinson, M. Zepf, S. Kar, R. Evans, and C. Bellei, “Radiation pressure acceleration of thin foils with circularly polarized laser pulses,” *New journal of Physics* **10**, 013021 (2008).
- <sup>10</sup>S. Bulanov, E. Esarey, C. Schroeder, S. Bulanov, T. Z. Esirkepov, M. Kando, F. Pegoraro, and W. Leemans, “Radiation pressure acceleration: The factors limiting maximum attainable ion energy,” *Physics of plasmas* **23**, 056703 (2016).
- <sup>11</sup>N. M. Bulgakova, A. V. Bulgakov, and O. F. Bobrenok, “Double layer effects in laser-ablation plasma plumes,” *Physical Review E* **62**, 5624 (2000).
- <sup>12</sup>A. M. Elsied, N. C. Termini, P. K. Diwakar, and A. Hassanein, “Characteristics of ions emission from ultrashort laser produced plasma,” *Scientific reports* **6**, 1–10 (2016).
- <sup>13</sup>P. Sankar, H. Shashikala, and R. Philip, “Ion dynamics of a laser produced aluminium plasma at different ambient pressures,” *Applied Physics A* **124**, 1–7 (2018).
- <sup>14</sup>N. Singh, M. Razafinimanana, and A. Gleizes, “The effect of pressure on a plasma plume: temperature and electron density measurements,” *Journal of Physics D: Applied Physics* **31**, 2921 (1998).
- <sup>15</sup>J. Thomas, H. C. Joshi, A. Kumar, and R. Philip, “Observation of ion acceleration in nanosecond laser generated plasma on a nickel thin film under rear ablation geometry,” *Physical Review E* **102**, 043205 (2020).
- <sup>16</sup>D. Wu, X. Mao, G. C.-Y. Chan, R. E. Russo, V. Zorba, and H. Ding, “Dynamic characteristics of multi-charged ions emitted from nanosecond laser produced molybdenum plasmas,” *Journal of Analytical Atomic Spectrometry* **35**, 767–775 (2020).
- <sup>17</sup>A. Batool, S. Bashir, A. Hayat, M. Akram, K. Mahmood, M. Javed, F. Hussain, S. H. Butt, H. Ahmad, Z. Irfan, *et al.*, “Time of flight measurements of energy and density of laser induced mg plasma ions and investigation of ablated surface morphology,” *Physics of Plasmas* **28**, 013113 (2021).
- <sup>18</sup>R. C. Issac, P. Gopinath, G. K. Varier, V. Nampoouri, and C. V. Labhan, “Twin peak distribution of electron emission profile and impact ionization of ambient molecules during laser ablation of silver target,” *Applied physics letters* **73**, 163–165 (1998).
- <sup>19</sup>B. Verhoff, S. Harilal, and A. Hassanein, “Angular emission of ions and mass deposition from femtosecond and nanosecond laser-produced plasmas,” *Journal of Applied Physics* **111**, 123304 (2012).
- <sup>20</sup>T. Kelly, T. Butler, N. Walsh, P. Hayden, and J. Costello, “Features in the ion emission of cu, al, and c plasmas produced by ultrafast laser ablation,” *Physics of Plasmas* **22**, 123112 (2015).
- <sup>21</sup>A. Dogar, S. Ullah, H. Qayyum, Z. Rehman, and A. Qayyum, “Characterization of charge and kinetic energy distribution of ions emitted during nanosecond pulsed laser ablation of several metals,” *Journal of Physics D: Applied Physics* **50**, 385602 (2017).
- <sup>22</sup>M. U. A. Bhatti, S. Bashir, A. Hayat, K. Mahmood, R. Ayub, M. Javed, and M. S. Khan, “Energy and flux measurements of laser induced silver plasma ions by using faraday cup,” *Plasma Science and Technology* (2021).
- <sup>23</sup>N. Farid, S. Harilal, H. Ding, and A. Hassanein, “Kinetics of ion and prompt electron emission from laser-produced plasma,” *Physics of Plasmas* **20**, 073114 (2013).
- <sup>24</sup>S. A. Irimiciuc, S. Chertopalov, J. Lancok, and V. Craciun, “Langmuir probe technique for plasma characterization during pulsed laser deposition process,” *Coatings* **11**, 762 (2021).
- <sup>25</sup>A. Kumar, R. Singh, J. Thomas, and S. Sunil, “Parametric study of expanding plasma plume formed by laser-blow-off of thin film using triple langmuir probe,” *Journal of Applied Physics* **106**, 043306 (2009).
- <sup>26</sup>S. Harilal, C. Bindhu, R. C. Issac, V. Nampoouri, and C. V. Labhan, “Electron density and temperature measurements in a laser produced carbon plasma,” *Journal of Applied Physics* **82**, 2140–2146 (1997).